Surface Science 102 (1981) 185–206

HARTREE–FOCK–SLATER–LCAO STUDIES OF THE ACETYLENE–TRANSITION METAL INTERACTION
I. Chemisorption on Ni surfaces; cluster models

Petro GEURTS and Ad VAN DER AVOIRD

Institute of Theoretical Chemistry, University of Nijmegen, Toernooiveld, Nijmegen, The Netherlands

Received 21 April 1980; accepted for publication 25 June 1980

The interaction of C_2H_2 with Ni surfaces has been studied by the Hartree–Fock–Slater–LCAO method (with core pseudopotentials). Different adsorption sites (π, di-σ, μ_2, μ_3) at the Ni(111) surface have been modelled by clusters of 1 to 4 Ni atoms; the structure of C_2H_2 and the Ni–C distance have been varied (3 structures, 2 distances). The acetylene–metal bonding can be interpreted in terms of π to metal donation and, especially, metal to π^* back donation effects which considerably weaken the C–C bond. These effects become increasingly important when more metal atoms are directly involved in the adsorption bonding: $\pi <$ di-$\sigma < \mu_2 < \mu_3$. The calculated shifts in the ionization energies are in fair agreement with the experimentally observed shifts (by UPS) for C_2H_2 adsorbed on Ni(111) (and other Ni surfaces); these shifts do not depend very sensitively on the bonding situation, however, so that we could not assign the structure of adsorbed C_2H_2 solely on this basis. From the comparison between the measured C–C stretch frequency (by ELS) and the calculated C–C overlap populations, using a relation calibrated on Ni–acetylene complexes, we find that μ_3 bonding of C_2H_2 with a Ni–C distance of about 1.9 Å is most probable on the Ni(111) surface; the CCH angle is estimated to be somewhat smaller than 150°. We have suggested an explanation for the surface specific dissociation of C_2H_2: C_2 fragments (C–H bond breaking) have been observed on stepped Ni surfaces (at low temperature), CH fragments (C–C bond breaking) have been found on ideal surfaces (at higher temperatures).

1. Introduction

During the past few years much attention has been given to the adsorption and reaction of small organic molecules on films and single crystal surfaces of transition metals, mainly to get insight in the fundamental aspects of more complicated catalytic processes. A simple and at the same time interesting molecule in this respect is acetylene, while among the first row transition metals, nickel has been studied most with regard to the adsorption of acetylene.

Different experimental techniques have been used to study C_2H_2 adsorbed on Ni: field emission microscopy (FEM) [1], gas phase analysis [2], ultraviolet photoelectron spectroscopy (UPS) [3–7], low energy electron diffraction (LEED) [5,8–10], Auger electron spectroscopy (AES) [8,9], electron energy loss spectros-

copy (ELS) [11–16], temperature programmed desorption (TPD) [5,11,12] and measurements of work function changes [1,4,5,7,11,12]. From these studies follows that molecular adsorption takes place at low temperature ($T \approx 100$ K) on the low index planes, whereas dissociation products will form at higher temperatures ($T > 300$ K to 400 K) and higher coverages on these planes; on stepped surfaces fragmentation starts already at low temperature.

A first important question is: how is the molecular C_2H_2 bound to the nickel surface, what is its geometrical and electronic structure? The answer to this question will probably have some bearing upon the possibilities for dissociation, too. The experimental data alone do not provide a complete picture and, moreover, the conclusions based on these data have been different. Several attempts have been made to obtain additional insight via quantumtheoretical studies. Demuth and Eastman [17] and Demuth [7,18] have performed Hartree–Fock (HF) LCAO calculations on free C_2H_2 and C_2H_2 bound to one Be atom in order to observe the effect of distortions in the molecular geometry on the electron binding energies; they have used the results for the interpretation of the UPS spectra measured for adsorbed C_2H_2. Upton and Goddard [19] have optimized the geometry of C_2H_2 in contact with one Ni atom by means of GVB–CI calculations (minimizing the total energy). A HF–LCAO study of C_2H_2 interacting with a Ni atom at a fixed geometry has been performed by Itoh and Kunz [20]. Clusters of nickel atoms with adsorbed C_2H_2 have been studied by the semi-empirical Extended Hückel (EH) [21,22] and CNDO/2 [23] methods. Kasowski [24] has obtained energy bands for a layer of C_2H_2 molecules (without metal) by the LCMTO method. These studies and similar ones for C_2H_2 on Be [25], Mn [26], Fe [27,28] and Pt [29,30] are hampered by the following problems. On the one hand, the ab initio calculations consider only one (transition) metal atom (or none at all), while the binding of C_2H_2 to nickel surfaces probably takes place with two or three neighbouring metal atoms. On the other hand, the semi-empirical treatments are not sufficiently accurate to yield, for example, reliable electron binding energies which can be compared with UPS spectra.

Therefore, we have undertaken a systematic study of C_2H_2 interacting in different manners with 1, 2, 3 or 4 Ni atoms. Although we realize that more Ni atoms are necessary to represent all the characteristics of a Ni surface and to obtain, for instance, accurate adsorption energies, level broadenings etc., these few nickel atoms form a first representation of different possible adsorption sites. And, since we shall look mainly at the properties of the C_2H_2 molecule itself and their changes upon adsorption, a model which includes the directly interacting metal atoms will already show most of the features upon which we concentrate in this paper. Geometry distortions of C_2H_2 have been taken into account and two different metal–C_2H_2 distances have been considered. The method that we have used is the non-empirical spin-restricted Hartree–Fock–Slater (HFS)–LCAO method [31], which has shown to yield fairly reliable molecular properties, in particular ionization energies [32,33]. We have not only looked at the electronic structure of the molec-

ularly adsorbed C_2H_2 on Ni, but we have also suggested an explanation for the two different pathways of dissociative chemisorption, which have been found on ideal surfaces and on stepped surfaces, respectively [5,13,15,16]. The bonding of the dissociation products, the relation with C_2H_2 bound to mono- and dinuclear Ni complexes (containing other ligands as well), and the adsorption of C_2H_2 on different transition metals (Fe and Cu) are subjects of subsequent papers [34].

2. Method and calculations

The self-consistent HFS–LCAO method developed by Ros, Baerends and coworkers, has been described in detail elsewhere [31–33]. Its most important features are the local exchange approximation [35] (Xα, with α fixed at 0.7), the representation of the electron density by one-centre fit functions and the numerical integration of the matrix elements over the HFS operator. We have used the core pseudopotential version of the method [36] (without perturbation corrections, cf. ref. [37]), which treats the valence electrons in the Coulomb and exchange field of the frozen cores, with projectors assuring core-valence orthogonality. The atomic orbital basis consists of 3d, 4s and 4p orbitals on Ni, 2s and 2p on C and 1s on H, each represented by two Slater type orbitals (STO's, double zeta basis). Also the frozen core shells are represented by such double zeta STO's. The exponents have been taken from Clementi and Roetti [38] (for Ni from the $3d^8 4s^2\ ^3F$ state); the 4p functions on Ni have been given the same exponents as the 4s, while the exponents for the hydrogen 1s functions (0.783003 and 1.383180) are optimal atomic HFS values. For the density fit functions one also uses STO's; we have included all angular functions (s-, p-, d-, f- and g-type) required by the AO basis, i.e. no spherical averaging of the density or the potential takes place (in contrast with the scattered wave implementation of the HFS method [39]). A somewhat more extended basis set has also been tested on the free C_2H_2 molecule, but this had hardly any effect on the electron binding energies and populations. The HFS–LCAO method has shown to yield rather good electronic properties for a number of small molecules and transition metal complexes, e.g. ref. [33], in particular also ionization energies. The core pseudopotential version has been tested on several atoms and diatomics [36] and on a fairly large transition metal cluster complex $[Fe_4S_4(SH)_4]^{2-}$ [37] *.

* The only problem with this version is that the energies of the virtual MO's are somewhat less accurate than those of the occupied ones. In large complexes with sets of nearly degenerate MO's, one finds sometimes, after iteration, empty orbitals lying slightly lower than the highest occupied ones, but this may occur also in HFS calculations without pseudopotential. Different occupancies lead to the same situation; the differences in the total energy are too small (in view of the accuracy of the latter) to make a definite choice. In our application to C_2H_2 adsorbed on Ni clusters, this causes the problem that we can not determine with certainty which of the orbitals around the Fermi level should be occupied. This problem only concerns the nearly degenerate anti-bonding metal orbitals, however, and we have always checked, in cases of doubt, that the different possible occupancies do not lead to any significant difference in the results for C_2H_2 adsorption.

SITE GEOMETRIES

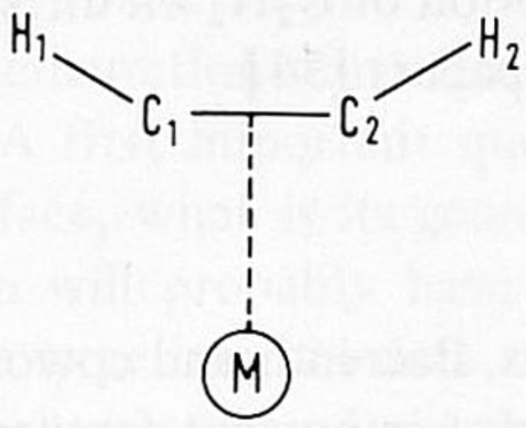

	$\angle_{CCH}$ (degr.)	180	150	120
	C–C (Å)	1.204	1.271	1.337
	C–H (Å)	1.056	1.071	1.086
π	M–$C_{1,2}$ (Å)	1.897	1.908	1.919
		2.405	2.413	2.422

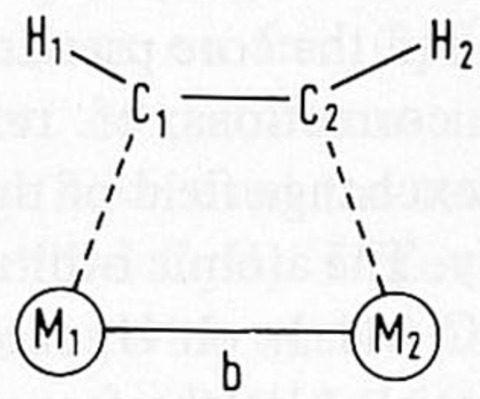

di–σ	$M_1–C_1 = M_2–C_2$ (Å)	1.911	1.900	1.890
		2.416	2.407	2.399

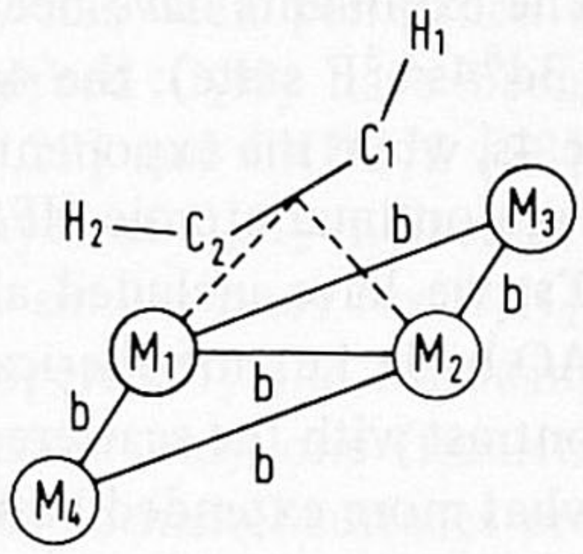

M_1+M_2	: μ_2			
$M_1+M_2+M_3$	: $\mu_{2(+1)}$			
$M_1+M_2+M_3+M_4$	: $\mu_{2(+2)}$			
	$M_{1,2}–C_{1,2}$ (Å)	1.897	1.908	1.919
		2.405	2.413	2.422
	$M_3–C_1 = M_4–C_2$ (Å)	2.026	2.001	1.976

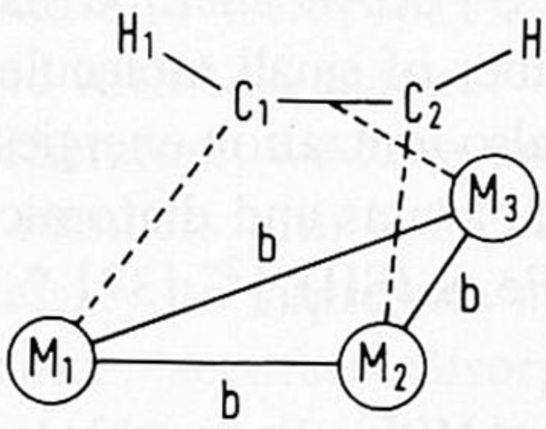

μ_3	$M_1–C_1 = M_2–C_2$ (Å)	1.911	1.900	1.890
		2.416	2.407	2.399
	$M_3–C_{1,2}$ (Å)	1.897	1.908	1.919
		2.405	2.413	2.422

Fig. 1. Model clusters for different C_2H_2 adsorption sites. For Ni the bulk nearest neighbour distance [52] is: b = 2.492 Å. The plane of (bent) C_2H_2 is always perpendicular to the metal surface plane. The metal-carbon distances are essentially 1.9 and 2.4 Å as described in the text. Small differences are caused by the changes in the C–C distance upon distortion of the C_2H_2 molecule, at constant height above the "surface".

From structure determinations of transition metal complexes, it has been found that C_2H_2 (or substituted acetylenes) can bind in several manners to one, two, three or four transition metal atoms [40–47]. Analogous binding sites have been pro-

posed for C_2H_2 on transition metal surfaces [5,11,12,14,21–23,29,30,48–51] and the Ni clusters which we have considered, see fig. 1, actually model these sites on the Ni(111) surface (some of them occur on other planes too). The μ_2 binding can be understood as a double π bond, each of the two perpendicular acetylene π orbitals interacting with one metal atom. The μ_3 bond can be imagined as a superposition of a π bond, for one of the acetylene π orbitals, and a di-σ bond, for the other π orbital. The interaction between each π orbital of acetylene and the metal can be interpreted in terms of the well known Dewar–Chatt–Duncanson model [53,54], which involves π to metal donation and metal to π^* back donation of electrons.

The nickel–carbon distance in our models was taken to be about 1.9 Å, which corresponds to the value observed in nickel–alkyne complexes [40–45]; in most cases we have also studied a distance of about 2.4 Å, which has been derived from the LEED analysis of the metastable C_2H_2 species on Pt(111) [49] (distance reduced by 0.1 Å for Ni). Acetylene has been distorted from a linear molecule (with the free molecule bond distances [52]) to a bent one with CCH angles of 150° and 120°. In the 120° case the C–C and C–H bond lengths of ethylene [55] have been used, in the 150° case they are obtained by linear interpolation. In the model for μ_2 bonding, we have added also one or two extra metal atoms to the cluster, $\mu_{2(+1)}$ and $\mu_{2(+2)}$, in order to observe their effects.

The questions, which are the preferred adsorption sites for C_2H_2 on Ni surfaces and what are the geometries of the adsorbed molecules, could in principle be answered on the basis of total (adsorption) energy calculations. The differences are probably very subtle, however, and the computations would become very time-consuming since many structural parameters may have to be relaxed in order to find maximum binding energy. It is worthwile to explore this approach in further studies, using procedures [56] which greatly improve the accuracy of the HFS binding energy calculations. In the present work, the calculated (adsorption) binding energies adopt unrealistic values due to numerical problems and we have chosen a different procedure. The results of our calculations for the different adsorption sites, different C_2H_2 distortions and different metal–carbon distances have been compared with the UPS and ELS data measured for C_2H_2 adsorbed on Ni. Ionization energies (corresponding with peak positions in UPS) can be calculated within the HFS scheme by the transition state method [32,35]. Vibrational frequencies (measured by ELS) can be compared with calculated force constants, but the direct computation of the latter is hard since it implies the knowledge of the total energy surface. Instead, we have used the almost linear relationship which has been found [57] between molecular stretch frequencies and calculated Mulliken [58,59] atom–atom overlap populations. This relation has been calibrated for the C–C stretch in acetylene by means of HFS calculations on nickel complexes with C_2H_2 as a ligand [34, paper III] and comparison with infrared frequencies. The correlation between our results calculated for the different structures and the measured UPS and ELS spectra has been used to indicate the most probable structure of C_2H_2 on Ni(111).

3. Results

3.1. Free acetylene

Acetylene in its ground state has the valence electron configuration $2\sigma_g^2 2\sigma_u^2 3\sigma_g^2 1\pi_u^4$. The $2\sigma_g$ orbital is primarily a C–C (2s–2s) bonding MO, the $2\sigma_u$ an odd combination of C–H bonding orbitals; $3\sigma_g$ is C–H bonding and C–C bonding (with more 2p character on C). Fig. 2 shows the valence MO schemes from ground and transition state calculations on free C_2H_2 (CCH angle 180°), together with the experimental ionization energies measured by UPS [18,60]. We observe that the transition state results are in fairly good absolute agreement with experiment. A similar agreement is found for the levels from the ground state calculation if we look at the relative positions (in the figure these levels are shifted, by –5.2 eV, to bring the $3\sigma_g$ level at the correct position). Apparently, the relaxation effect on the

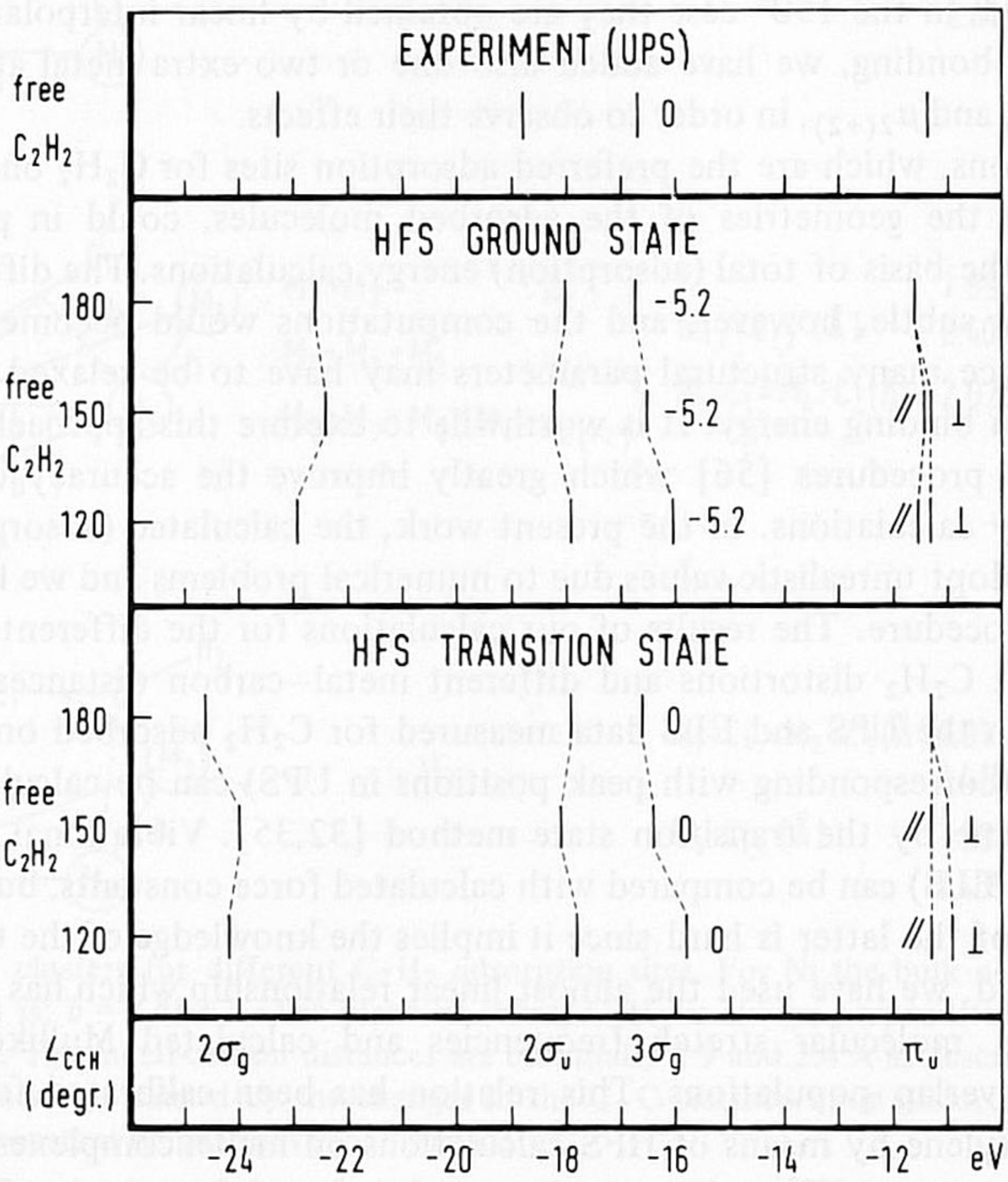

Fig. 2. Acetylene MO schemes from HFS ground state and transition state calculations, compared with the experimental (UPS) ionization energies [18,60]. The ground state spectra have been shifted (by the amount indicated in eV) in order to bring the $3\sigma_g$ level of free C_2H_2 (CCH angle 180°) to the same position as the experimental level.

different ionization energies is rather uniform, except for the lower lying $2\sigma_g$ orbital. In spite of this satisfactory agreement, the deviations between the calculated and the experimental values are of the same magnitude as the ionization energy shifts observed upon adsorption. Therefore, we shall look in the next section at the adsorption shifts in the calculated and experimental levels, rather than at the level positions.

Fig. 2 also shows the effects of geometry distortion of the C_2H_2 molecule on the calculated ionization energies. These effects are almost identical in the ground and transition states. The π orbital in the plane of bending * is destabilized more than the one perpendicular to it. Also the $2\sigma_g$ and $3\sigma_g$ levels are destabilized, but the $2\sigma_u$ level is stabilized at the CCH angle of 150°; for 120° the picture changes again.

From the population analysis [58,59] in table 1 it follows that the C_2H_2 bending causes a charge shift from the C–C overlap population to the net atomic C populations, while the other populations remain almost unaffected. This can be understood since the C_2H_2 bending is accompanied by an increase in the C–C bond length, which is substantially larger than the increase of the C–H bond length.

3.2. Adsorbed acetylene: ionization energies, relation with UPS

The ionization energies, I_{ads}, measured for an adsorbed molecule can be related to the free molecule ionization energies, I_{free}, by the following expression (i labels the different ionized states):

$$I^i_{ads} = I^i_{free} + \Delta E^i \ .$$

Experimentally, the ionization energies I_{ads} are measured relative to the work function of the substrate–adsorbate system, which can be written as the clean metal work function, ϕ, plus changes, $\Delta\phi$, caused by adsorption. The ionization energy shift ΔE^i is often thought to be composed of two components: $\Delta E^i = \Delta E^i_b + \Delta E^i_r$. This decomposition is related to the interpretation of the ionization energy as a molecular orbital energy (Koopmans' theorem [61]) plus a relaxation energy, caused by the relaxation of the orbitals of the ion. The bonding (initial state) shift ΔE^i_b is then the change in that molecular orbital energy upon adsorption, due to the interaction with the metal. The relaxation (final state) shift ΔE^i_r is the difference in relaxation energy between the free ion and the adsorbed ion, mainly caused by the screening or partial filling of the electron hole by the metal electrons. In the HFS method, which we have used, Koopmans' theorem does not hold, so, formally, we cannot make this distinction. The total shifts ΔE^i can be obtained from the molecular orbital levels in transition state calculations. Still, we can also use the

* Note that this orbital is indicated as $\pi_\perp$ since, upon adsorption, it is the one perpendicular to the surface. The π orbital perpendicular to the plane of the bent C_2H_2, but parallel to the surface, is indicated as $\pi_{/\!/}$.

Table 1
Population analysis for free C_2H_2

		CCH angle (deg)		
		180°	150°	120°
Net atomic populations	C	3.00	3.18	3.41
	H	0.30	0.31	0.32
Gross atomic charges	C	−0.32	−0.33	−0.34
	H	0.32	0.33	0.34
Atom–atom overlap populations	C–C	1.89	1.59	1.21
	C–H	0.75	0.74	0.73

relative positions of the ground state MO levels, if the transition state relaxation effects in the HFS calculations (which should not be confused with ΔE_r^i defined above) are the same for the different levels. In the free molecule this has been found, except for the lowest valence level, $2\sigma_g$ (see section 3.1).

In figs. 3 to 6 we have shown the ground state and transition state MO levels calculated for (distorted) C_2H_2 on different adsorption sites. The interactions between C_2H_2 and the metal are not so strong that we cannot distinguish the pure C_2H_2 MO's anymore. We have drawn only those levels which are primarily composed of the occupied valence MO's of C_2H_2 *; these levels happen to be the lowest occupied valence orbitals in all adsorption clusters. Since we want to look at the adsorption shifts ΔE^i, we have included the diagrams for free, undistorted C_2H_2 and the experimental UPS data for free C_2H_2 [18,60] and C_2H_2 adsorbed on Ni(111) [5–7,18]. These shifts are taken relative to the shift of the $3\sigma_g$ level, as in other interpretations of the UPS spectrum [4–7,17,18,22], but the shifts of this $3\sigma_g$ level (and thus of the whole MO schemes) are also indicated in the figures.

First we conclude that the transition state calculations compared to the corresponding ground state results, show the same behaviour as for free C_2H_2: all levels exhibit a practically uniform relaxation effect, except the $2\sigma_g$ orbital again. So, indeed, we can use the ground state MO schemes to obtain the adsorption shifts in the upper valence levels.

The next conclusion we can draw is that, contrary to the assumption by Demuth et al. [7,17,18], the adsorption shifts ΔE^i are very different from the shifts caused by the distortion of the free acetylene molecule, even for the σ levels. The largest (bonding) shifts are found for the π_u levels and these shifts are in the opposite direction from the effects of the distortion alone. Also the splitting between the $\pi_\perp$ and $\pi_{/\!/}$ levels is in the opposite sense, in most cases, and this is quite understandable if we look at the reason for the π level stabilization, the bonding interaction with the nickel atoms, and at the geometries of the adsorbate–metal systems. The

* We have also used the same symbols as in the free C_2H_2 molecule to denote these MO's.

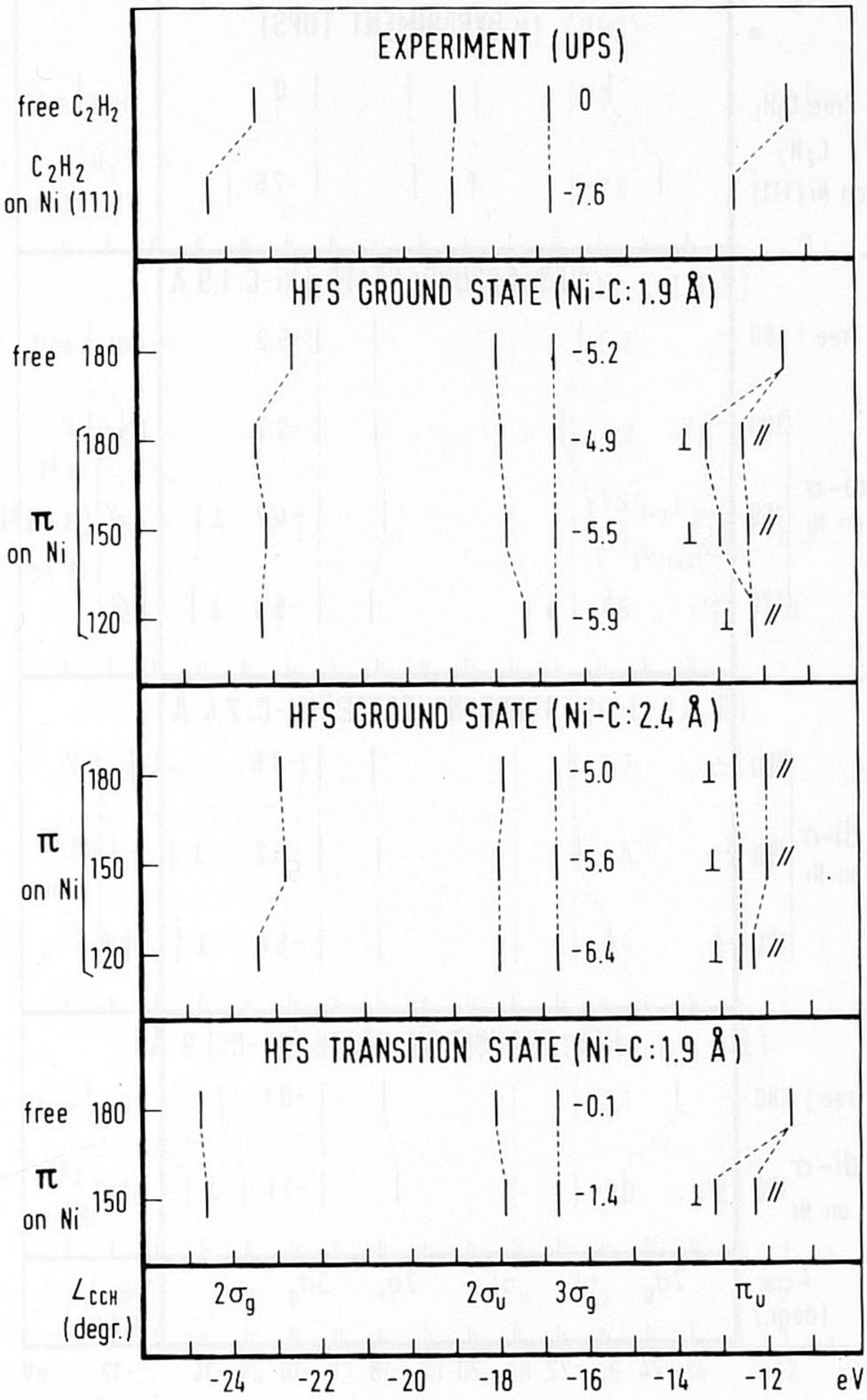

Fig. 3. MO schemes for C_2H_2 on the Ni π site from HFS ground state and transition state calculations, compared with the free C_2H_2 level schemes. The same comparison is made for the experimental (UPS) ionization energies of C_2H_2 molecularly adsorbed on Ni(111) [5–7,18] (measured relative to the work function) and the ionization energies of free C_2H_2 [18,60]. All spectra have been shifted by the amount indicated (in eV) next to the $3\sigma_g$ levels in order to bring these $3\sigma_g$ levels into the same position.

$\pi_\perp$–$\pi_{/\!/}$ splitting is largest if only one π orbital ($\pi_\perp$) is involved in the (σ-type) bonding to the metal (as for the π site, but especially for di-σ bonding). When both the π orbitals of acetylene are involved (μ_2, μ_3 bonding), this splitting is somewhat smaller. This can be understood if we transform the $\pi_\perp$ and $\pi_{/\!/}$ orbitals, which obey

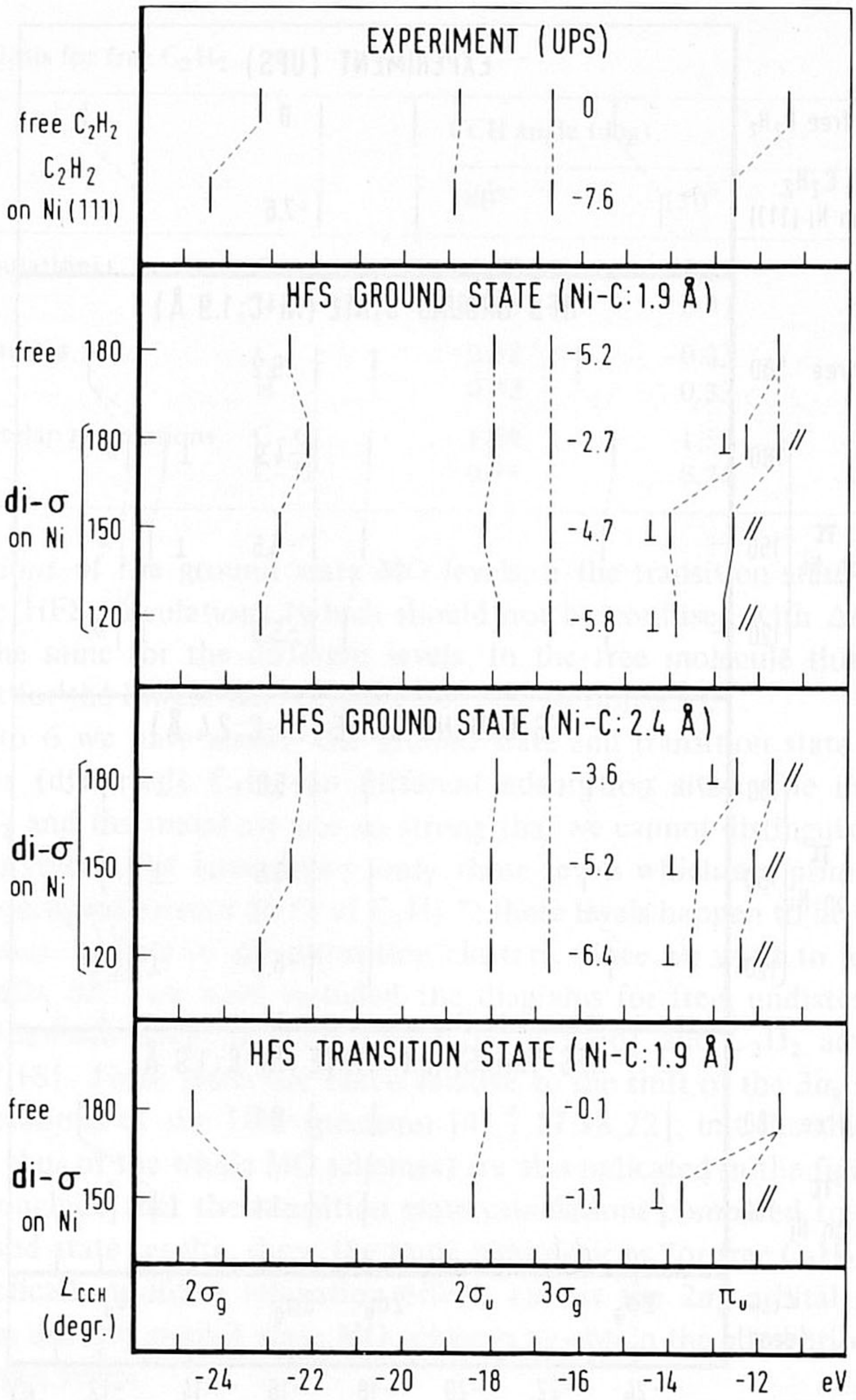

Fig. 4. MO schemes for C_2H_2 on the Ni_2 di-σ site; see further the caption of fig. 3.

the symmetry of the cluster models (fig. 1), to a new set of two rotated π orbitals which point directly to the metal atoms (such a transformation leaves the total wave function invariant if both π orbitals are doubly occupied). In the μ_2 cluster, where these new π orbitals are completely equivalent, the $\pi_\perp$–$\pi_{/\!/}$ splitting is only due to the interaction between the equivalent π-to-metal bonds and to the distortion of C_2H_2 in the 150° and 120° cases.

The overall picture for the upper valence levels that emerges from the UPS spec-

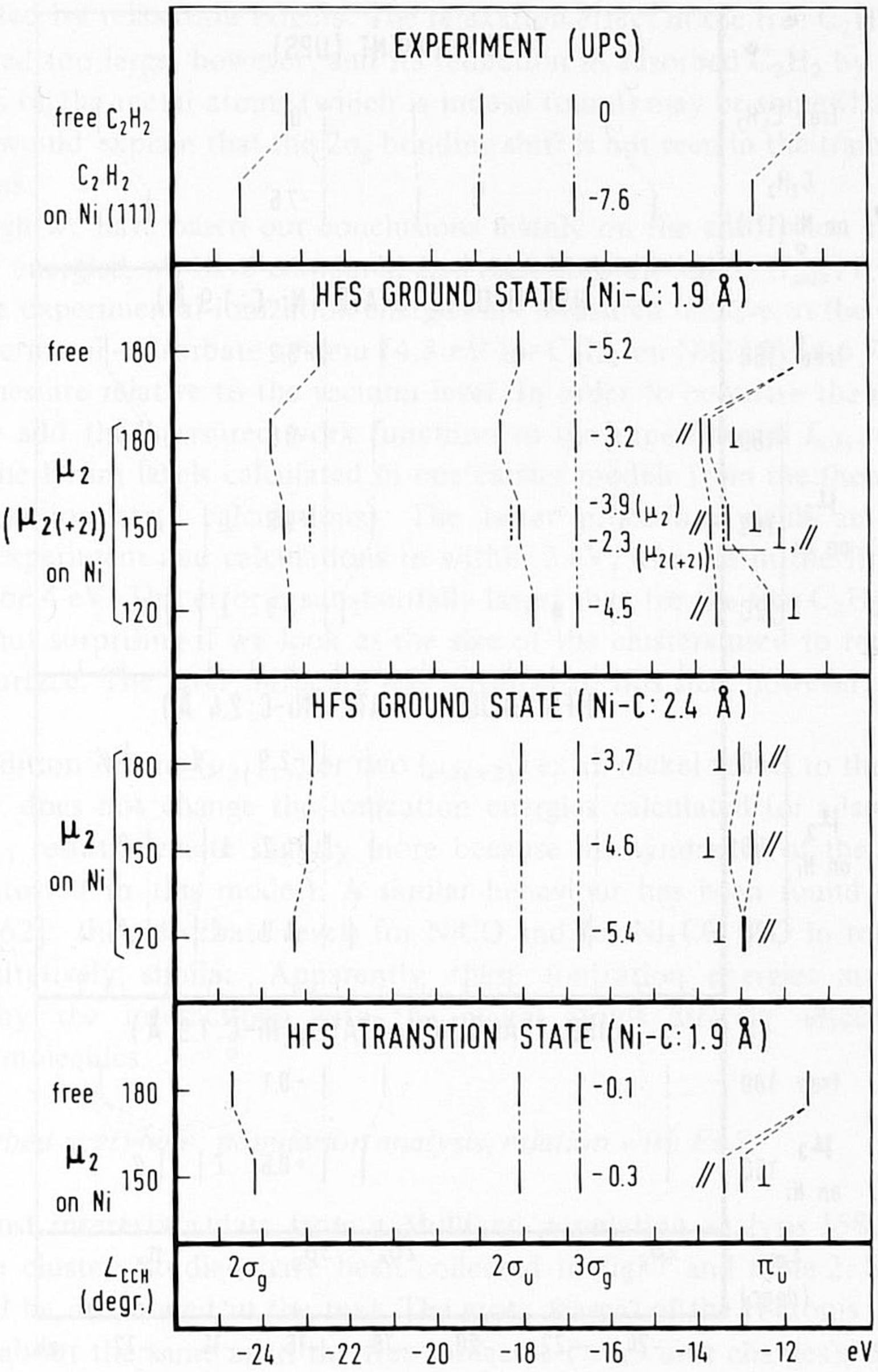

Fig. 5. MO schemes for C_2H_2 on the Ni_2 μ_2 and Ni_4 $\mu_{2(+2)}$ (dashed bars) sites; see further the caption of fig. 3.

trum of C_2H_2 on Ni(111), i.e. a small change in the $2\sigma_u$–$3\sigma_g$ splitting and a relatively large bonding shift of the π_u levels, is found in many of the models calculated. Also the $\pi_\perp$–$\pi_\parallel$ splitting is small enough in various cases to explain the single broadened π_u ionization feature observed. An interesting detail, in this respect, is that, some years ago, two distinct π_u levels with a splitting of about 2 eV have been measured for C_2H_2 on polycrystalline Ni [3]. A definite assignment of the structure

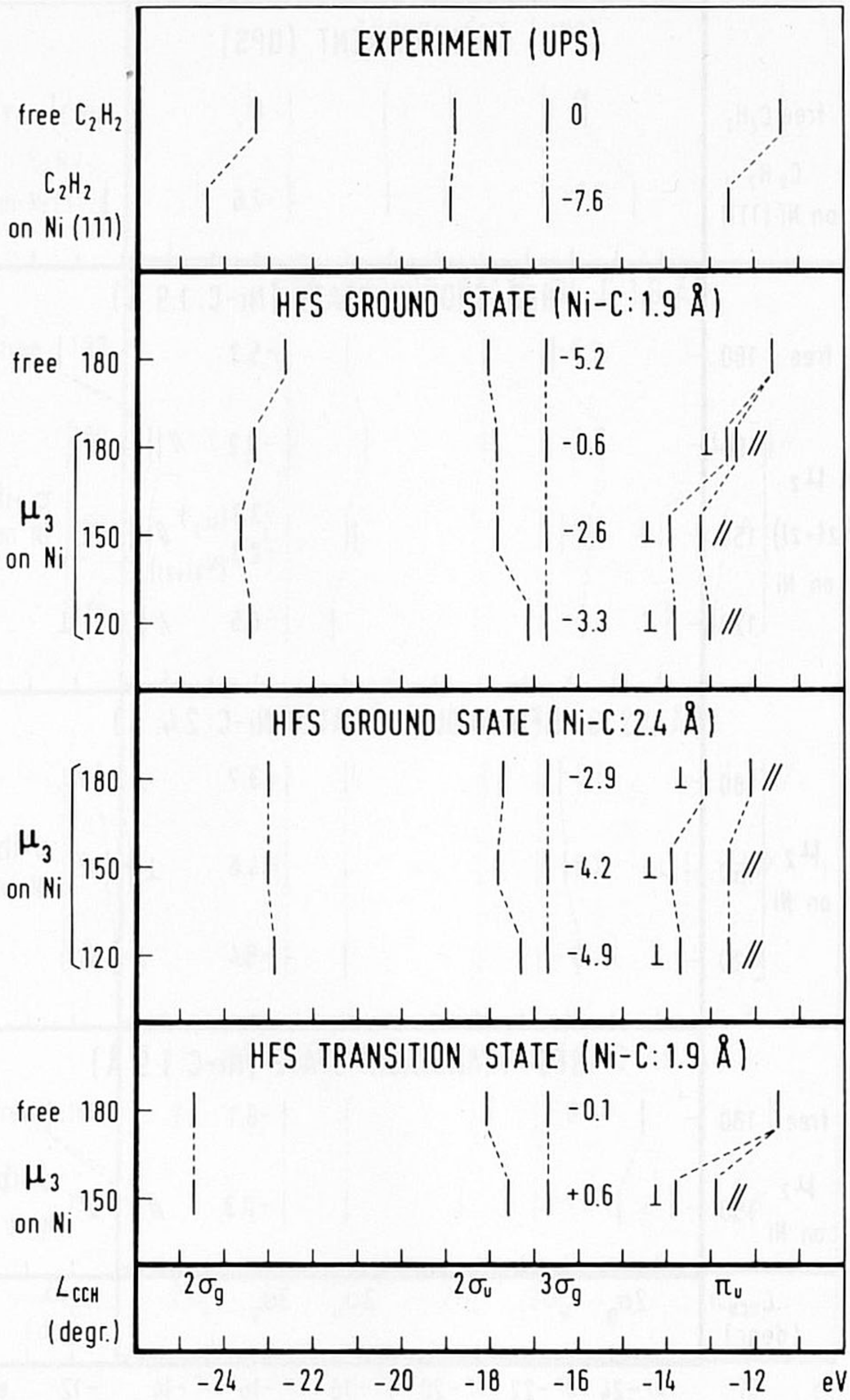

Fig. 6. MO schemes for C_2H_2 on the Ni_3 μ_3 site; see further the caption of fig. 3.

and the bonding site of C_2H_2 on Ni(111) cannot be made, however, because the differences between the results calculated for different situations are too small, with respect to the deviations from the experimental UPS spectrum which are still present. We shall come back to this point in section 4 when we have discussed the calculations related to the ELS spectrum.

The (bonding) shift of the $2\sigma_g$ level, which has been measured, is only found in some of the ground state calculations. In the transition state results this shift is

compensated by relaxation effects. The relaxation effect in the free C_2H_2 molecule is calculated too large, however, and its reduction in adsorbed C_2H_2 by the screening effects of the metal atoms (which is indeed found) may be somewhat too large also; this would explain that the $2\sigma_g$ bonding shift is not seen in the transition state calculations.

Although we have based our conclusions mainly on the adsorption shifts in the ionization energies, we have compared also their absolute values (I_{ads}) for adsorbed C_2H_2. The experimental ionization energies are measured relative to the work function of the metal–adsorbate system (4.3 eV for C_2H_2 on Ni(111) [4,5,7]), the calculated ones are relative to the vacuum level. In order to compare the results, one can either add the measured work functions to the experimental I_{ads}, or one can subtract the Fermi levels calculated in our cluster models from the theoretical I_{ads} (from transition state calculations). The latter procedure yields an agreement between experiment and calculations to within 2 eV, whereas in the first case the error can be 4 eV. This error is substantially larger than for the free C_2H_2 molecule, which is not surprising if we look at the size of the clusters used to represent the Ni(111) surface. The level shifts are less sensitive to this size, however, as we have checked.

The addition of one ($\mu_{2(+1)}$) or two ($\mu_{2(+2)}$) extra nickel atoms to the μ_2 cluster practically does not change the ionization energies calculated for adsorbed C_2H_2 (the $\mu_{2(+1)}$ results deviate slightly more because the symmetry of the adsorption site is distorted in this model). A similar behaviour has been found for CO on Ni(100) [62]: the adsorbate levels for NiCO and for Ni_5CO (CO in top position) are quantitatively similar. Apparently these ionization energies are primarily affected by the interactions with the nickel atoms directly adjacent to the adsorbate molecules.

3.3. Adsorbed acetylene: population analysis, relation with ELS

The most interesting data from a Mulliken population analysis [58,59] of the adsorption clusters studied have been collected in fig. 7 and table 2. Some other results will be mentioned in the text. The gross charges of the H atoms in adsorbed C_2H_2 are about the same as in the free molecule ($\simeq$0.3 unit charges); the C atoms have acquired some extra negative charge, however, which ranges from –0.2 to –0.6 unit charges (increasing with distortion angle and in the order π, di-$\sigma < \mu_2 < \mu_3$). This negative charge on the adsorbed C_2H_2 molecule, which has been found also from an ab initio HF–LCAO study of C_2H_2 interacting with one Ni atom [20], seems in contradiction with the measured work function lowering [1,4,5,7,11,12]. This comparison is based, however, on a simple surface dipole layer model for the work function change. Maybe this model is not applicable in this case; it has been questioned for C_2H_2 adsorption on a Pt surface also [63]. Another explanation could be that the Mulliken population analysis, which makes a rather arbitrary assignment of the charge to the overlapping orbitals, not corresponding to any

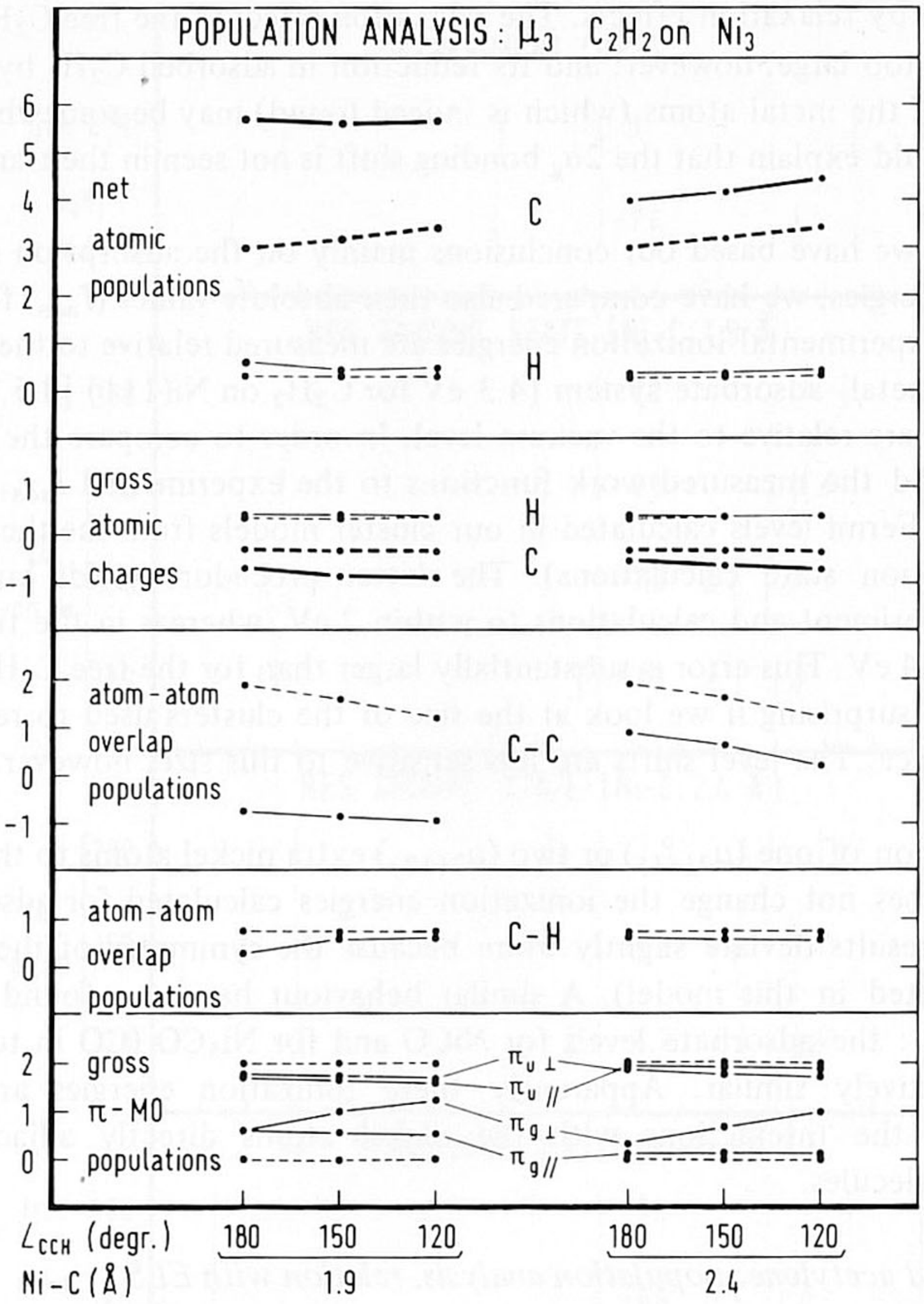

Fig. 7. Population analysis data for C_2H_2 on the Ni_3 μ_3 site (solid lines), compared with free C_2H_2 results (dashed lines).

physically observable quantity, does not properly reflect the spatial (re)distribution of charge. The total dipole moments calculated for our C_2H_2–metal clusters point with their positive parts away from the metal in some cases, whereas the total Mulliken charge on C_2H_2 is always negative. Also these dipole moments cannot be trusted, however, for an explanation of the observed work function change, since the metal clusters are too small; this leads to artificial edge effects.

The calculated extra charge on the C atoms mainly originates from the Ni 4s orbitals of which the gross populations decrease from about 2.0 to about 1.0 electrons in the series π to μ_3. There is also a (slight) increase in the Ni 3d gross populations from 7.4 to 8.0 electrons, while the amount of Ni 4p electrons is almost constant, about 0.6 (except for the π site where it is 0.2). How this extra charge on the

C_2H_2 molecule is accomodated we can see by looking at the populations of the π_u orbitals and their antibonding π_g^* counterparts. These MO (gross) populations have been defined by a transformation of the populations from the AO basis to the MO's of (distorted) C_2H_2, using the MO coefficients of the free C_2H_2 molecule. We observe from table 2 and fig. 7 that there is some donation of electrons from the occupied π_u orbitals of acetylene to the metal orbitals. The back donation of metal electrons to the unoccupied π_g^* orbitals of C_2H_2 is much larger, however, and this explains the negative charge on the carbon atoms. The donation–back donation effect increases in the order $\pi < \text{di-}\sigma < \mu_2 < \mu_3$ and also we observe that in the cases of μ_2 and μ_3 bonding both the $\pi_\perp$ and the $\pi_{/\!/}$ orbitals become involved. This is in agreement with the bonding shifts and the splitting between the π levels of C_2H_2 as discussed in section 3.2 (in terms of rotated π orbitals which point to the metal atoms). These π orbital populations can be used to define a type of (Mulliken) C–C bond order as the number of electrons in the bonding π_u orbitals minus the number of electrons in the antibonding π_g^* orbitals, divided by two. For free C_2H_2 this π bond order equals two, but it decreases to values smaller than one for μ_2 and μ_3 adsorption (see table 2). A parallel effect is found in the C–C atom–atom overlap population.

When the adsorbed C_2H_2 molecule is distorted we observe the same trend as in the free molecule: a growth of the C net atomic populations at the expense of the C–C overlap population; the absolute value of the latter is much smaller, however, and the C net populations are larger, due to the interaction with the metal atoms (donation–back donation) which we have just discussed. The increase of π^* back donation with increasing distortion angle can (at least in part) be understood from the stabilizing influence of bending on the receiving π_g^* orbitals; in free C_2H_2 the one-electron energies of $\pi_{g\perp}^*$ and $\pi_{g/\!/}^*$ change from +1.39 eV at the CCH angle of 180°, via −1.08 eV ($\pi_{g\perp}^*$) and +0.62 eV ($\pi_{g/\!/}^*$) at 150°, to −3.25 eV ($\pi_{g\perp}^*$) and −0.04 eV ($\pi_{g/\!/}^*$) at 120°. From these values the generally better acceptor ability of $\pi_{g\perp}^*$ compared to $\pi_{g/\!/}^*$ can be explained too (in combination with geometry arguments). The fact that distortion does not have such a pronounced effect on the π_u levels, explains the small variation of π donation as a function of distortion angle; probably geometry arguments are solely important to explain that $\pi_{u\perp}$ donates better than $\pi_{u/\!/}$. Naturally, the donation–back donation interactions increase with decreasing Ni–C distance (from 2.4 to 1.9 Å). The C–H overlap populations decrease only slightly, except for the $\mu_{2(+1)}$ and $\mu_{2(+2)}$ adsorption models.

In the $\mu_{2(+1)}$ and $\mu_{2(+2)}$ cases they decrease considerably, e.g. to about −2.49 for $\mu_{2(+1)}$ for the linear adsorbed C_2H_2, compared with the free molecule value of 0.75. This must be due to an extremely strong interaction with the extra nickel atoms (in the $\mu_{2(+1)}$ cluster it happens only at the side of C_2H_2 near the added Ni atom). We can expect this effect if we look at the distances between the H atoms and the extra nickel atoms: 1.39 Å, compared with an estimated sum of Van der Waals radii larger than 2.4 Å. When the C_2H_2 molecule is distorted to a CCH angle of 150° (Ni–H distance 1.93 Å), this interaction diminishes and the C–H overlap

Table 2
Selected population analysis data for C_2H_2 on Ni clusters

Site	CCH angle (deg)	C–C overlap population		Gross π-MO population			
				$\pi_{u\perp}$		$\pi_{u\parallel}$	
	Ni–C (Å)	1.9	2.4	1.9	2.4	1.9	2.4
π	180	1.03	1.39	1.77	1.88	1.92	1.97
	150	0.69	0.92	1.78	1.87	1.91	1.97
	120	0.40	0.55	2.04	2.00	1.89	1.96
di-σ	180	0.69	1.28	1.73	1.88	1.91	1.97
	150	0.61	0.88	1.66	1.83	1.88	1.95
	120	0.36	0.52	1.79	1.88	1.84	1.93
μ_2	180	0.16	1.18	1.75	1.88	1.70	1.86
	150	−0.10	0.66	1.68	1.80	1.66	1.81
$(\mu_{2(+2)})$	(150)	(0.02)		(1.67)		(1.59)	
	120	−0.19	0.18	1.73	1.77	1.62	1.77
μ_3	180	−0.75	0.93	1.74	1.87	1.71	1.92
	150	−0.85	0.68	1.71	1.78	1.66	1.92
	120	−0.92	0.20	1.68	1.71	1.58	1.89

population is restored to the more realistic, but still low value of 0.11 for $\mu_{2(+2)}$ and 0.01 for $\mu_{2(+1)}$. Upon further distortion to 120° (Ni–H distance 2.41 Å) we find a C–H overlap population of 0.42 for $\mu_{2(+1)}$. We shall come back to these results when we discuss possible C_2H_2 dissociation mechanisms (section 4).

Now we relate the population data to the adsorption shifts in the C_2H_2 vibration frequencies measured by ELS [11,12,14]. From the ELS spectra for C_2H_2 on Ni(111) it has been found that the C–C stretch frequency, $\nu_{C\equiv C}$, is strongly lowered to 1218 cm^{-1} [11,12] or 1215 cm^{-1} [14] (free molecule value 1974 cm^{-1} [64]). By comparing these data to the C–C stretch frequencies for ethylene and ethane it has been concluded that the total ($\sigma + \pi$) C–C bond order should be about 1.15 and that the hybridization of the carbon atoms should be close to sp^3. The change in $\nu_{C\equiv C}$ is in agreement with our calculations (C–C overlap populations decrease considerably). We have also shown, however, that it is dangerous to draw conclusions about the properties of adsorbed C_2H_2 molecules by comparing the measured data with free molecule values, since the interaction with the metal changes the properties in a way which cannot be imitated by considering free molecules. Still, it would be interesting to make a more quantitative comparison between the considerable reduction in the measured $\nu_{C\equiv C}$ and our calculated results for the different adsorption models. We have done this by performing HFS–LCAO calculations on some mono- and dinuclear Ni complexes with C_2H_2 as a ligand, π or μ_2 bonded, in combination with other ligands (isocyanide, carbonyl). For these

	$\pi^{\star}_{g\perp}$		$\pi^{\star}_{g\parallel}$		π donation		$\pi^{\star}$ back donation		π bond order	
	1.9	2.4	1.9	2.4	1.9	2.4	1.9	2.4	1.9	2.4
	0.57	0.35	0.11	0.02	0.31	0.15	0.68	0.37	1.51	1.74
	0.83	0.59	0.09	0.01	0.31	0.16	0.92	0.60	1.39	1.62
	1.00	0.82	0.08	0.01	0.07	0.04	1.08	0.83	1.43	1.57
	0.59	0.29	0.23	0.04	0.36	0.15	0.82	0.33	1.41	1.76
	0.84	0.65	0.18	0.03	0.46	0.22	1.02	0.68	1.26	1.55
	1.10	0.93	0.17	0.03	0.37	0.19	1.27	0.96	1.18	1.43
	0.48	0.22	0.57	0.16	0.55	0.26	1.05	0.38	1.20	1.68
	0.84	0.51	0.53	0.15	0.66	0.39	1.37	0.66	0.99	1.48
	(1.07)		(0.69)		(0.74)		(1.76)		(0.75)	
	1.07	0.81	0.50	0.11	0.65	0.46	1.57	0.92	0.89	1.31
	0.62	0.32	0.59	0.12	0.55	0.21	1.21	0.44	1.12	1.68
	1.02	0.68	0.58	0.11	0.63	0.30	1.60	0.79	0.89	1.46
	1.20	0.99	0.54	0.09	0.74	0.40	1.74	1.08	0.76	1.26

complexes the shifts in $\nu_{C\equiv C}$ have been measured by infrared spectroscopy. Our calculations show [34, paper III] that there exists an approximate linear relation between $\nu_{C\equiv C}$ and the total C–C overlap population. (A similar relation has been found for the C–O stretch in various carbonyl complexes [57], cf. also ref. [65].) From this relation, calibrated in paper III, and the ELS value $\nu_{C\equiv C} \simeq 1215$ cm^{-1}, we estimate the C–C overlap population for C_2H_2 adsorbed on Ni(111) to be around -0.55 ± 0.25 *. Results are calculated close to this value for μ_3 adsorption with a Ni–C distance of about 1.9 Å. From the calculations it also follows that the lowering of the C–C overlap population depends much more strongly on the interaction with the metal atoms than on the geometrical distortion of C_2H_2 itself.

4. Structure of adsorbed C_2H_2: bonding, site preference, dissociation mechanisms

We have found in the preceding sections that the interaction between a C_2H_2 molecule and a nickel surface, represented by a small collection of nickel atoms,

* Negative values for the overlap population seem strange if we think of this overlap population as a measure for the (absolute) bond strength. The Mulliken overlap population is not a physically observable quantity, however, and it has often been found [57] to be negative between atoms which are still chemically bonding. Its value depends on the choice of the AO basis set also. One may only relate changes in the overlap population, calculated within the same basis, with changes in the bond strength preferably after calibration, as we have done here.

takes place via the Dewar–Chatt–Duncanson [53,54] donation–back donation mechanism. Both, from the MO level shifts and from a population analysis we can conclude that mainly the acetylene π orbitals take part in this mechanism; the populations of the occupied $2\sigma_g$, $2\sigma_u$ and $3\sigma_g$ orbitals hardly change and also the relative σ level positions remain much more constant than the positions of the π levels. In the ground state HFS calculations we find, in some cases, a (small) bonding shift of the $2\sigma_g$ level, in agreement with experiment, but in the transition state results this shift is compensated by a (too large?) relaxation effect. The strength of the metal–acetylene interaction increases when more directly adjacent metal atoms take part in the bonding: $\pi <$ di-$\sigma < \mu_2 < \mu_3$. Especially in the latter two cases both the acetylene π orbitals cooperate in the bonding. We do not know, however, whether the adsorption energy also increases in this order, since we have not calculated accurate total energies.

Although the calculated adsorption shifts in the ionization energies agree fairly well with the shifts measured by UPS, the comparison of the UPS spectrum with the calculated ionization spectra is not sufficient to discriminate between all possible structures and binding sites for C_2H_2 on Ni(111). The calculated level schemes do not depend very sensitively on the bonding situation of C_2H_2 to the nickel atoms. (A similar conclusion has been made for CO on Ni(100) [62], where one could not distinguish between a top NiCO or Ni_5CO molecule and a fourfold hollow Ni_5CO binding site). Only certain situations (e.g. di-σ bonding) can be excluded, for example, because they yield a large $\pi_\perp - \pi_{/\!/}$ splitting, which has not been found experimentally.

From the comparison of the shifts in the calculated C–C overlap populations, $q_{C\equiv C}$, with the lowering of the C–C stretch frequency $\nu_{C\equiv C}$, found by ELS measurements, we can conclude, however, that C_2H_2 is bonded most probably in a threefold site (μ_3 bonding) on the Ni(111) surface, with a Ni–C distance of about 1.9 Å. This comparison can be made semi-quantitatively since we have found (and calibrated) an approximately linear relation between $\nu_{C\equiv C}$ and $q_{C\equiv C}$ in some Ni complexes with acetylene ligands. We cannot be sure about the geometric distortion of the C_2H_2 molecule, but since the $2\sigma_u - 3\sigma_g$ splitting does not change very much and the $\pi_\perp - \pi_{/\!/}$ splitting is rather small, we think that this distortion will be not much larger than 30° (CCH angle 150°). Values in this range have been found also in some nickel complexes [40–45] (CCH angles from 149° to 126°). A further indication comes from considering the experimental LEED structure [5,9,10], p(2 × 2), the phase to which also the UPS and ELS results correspond. The occurrence of μ_3 bonding implies internuclear distances between hydrogen atoms of adjacent C_2H_2 molecules which are 1.7, 1.9 and 2.5 Å for CCH angles of 180°, 150° and 120° respectively. Looking at the Van der Waals radius of H (1.2 Å [66]) we can practically rule out the undistorted linear C_2H_2 structure (Demuth [5] has argued on this basis, that μ_3 sites are excluded, since he assumed, at that time, that adsorbed C_2H_2 is almost linear). Combining the different pieces of information we estimate a CCH angle of somewhat less than 150°. Other studies [11,12,14,18],

which do not explicitly include the interaction with transition metal atoms, need still larger distortions to explain the experimental shifts.

Although the different properties calculated for μ_3 site adsorption fit the various experimental data rather nicely, we can, of course, not exclude that another structure holds, which we have not calculated. So, for instance, our calculations indicate that probably also μ_2 adsorption is rather stable. In this case, slightly extrapolating our results, the C_2H_2 molecule on Ni(111) would have to be distorted somewhat stronger in order to find a C–C overlap population agreeing with the ELS data. Again, the C–H groups are probably bent upwards by at least 30° in order to avoid too strong interaction between the H atoms and some of the Ni atoms, which would reduce the C–H overlap population too much (see section 3.3). Also it is possible that the C–C axis is not exactly parallel to the surface, but somewhat tilted [14] or that the C_2H_2 plane is not perpendicular to the surface [12]. Anyway, we can be rather sure that μ_2 type bonding will occur on other surfaces which have no threefold sites such as Ni(111). UPS data are available for molecular C_2H_2 adsorbed on Ni(100) and (110) surfaces [18], but the spectra are rather similar to the (111) results. This shows again the insensitivity of UPS spectra with regard to the exact binding site and structure. Because ELS data are lacking yet, we cannot make an analysis as described above.

Next, we discuss some results of our calculations in relation to the dissociation behaviour of C_2H_2. At somewhat higher temperatures and coverages ($T > 300$ to 400 K) it has been concluded from TPD experiments, LEED and UPS data [5] and from ELS measurements [13,16], that on Ni(111) C_2H_2 dissociates into (adsorbed) CH species. In the molecularly adsorbed C_2H_2 at low temperature one finds considerable lowering of the C–C stretch frequency already, but not the softening and broadening of the C–H stretch that is present in some other cases of adsorbed hydrocarbons which dehydrogenate at higher temperatures [67]. On a stepped Ni[5(111) × ($\bar{1}$10)] surface, ELS shows that dehydrogenation takes place, however, even at temperatures as low as 150 K, leaving adsorbed C_2 species [15,16]. This preference for C–C bond breaking in one case, and C–H scission in the other, is very interesting since it is a simple example of a surface specific dissociation process and it takes place at well defined surfaces at low pressure and temperature.

The picture of C–C bond breaking on the Ni(111) surface is consistent with our calculations for the μ_3 adsorption site: the C–C overlap population is strongly reduced, while the C–H value is only slightly smaller than in free C_2H_2. At other surfaces the situation will probably be different and μ_2 type bonding could occur. In that case one might have Ni atoms close to the hydrogen atoms just as in our $\mu_{2(+1)}$ and $\mu_{2(+2)}$ models for the (111) plane. Especially, if the molecules are adsorbed near steps we expect the presence of such extra Ni atoms. Our calculations show that the strong interactions between these additional metal atoms and the H atoms (or the C–H groups) can strongly reduce the C–H overlap populations. The C–H groups could bend away, leading to a restoration of the C–H bond, a further reduction of the C–C bond strength and eventually C–C scission again, but

it is also possible that the C–H bonds break first. The latter process would lead, in first instance, to C–C–H and C–C fragments. The C–C fragments will probably not be very stable on flat surfaces, however, since one expects both C atoms to bind to several nickel atoms, leading to a C–C axis nearly parallel to the surface, but the bond angles are rather unfavourable then (the bonds on the C atoms will point to the other C atom and to the surface, i.e. more or less to one side). At steps, we have metal atoms above the surface and the C–C fragments can easily accomodate themselves in positions with the carbon atoms having more favourable bond angles. Thus, we can tentatively explain the formation of C–C fragments from C_2H_2 on stepped Ni surfaces as being due to the presence of nickel atoms nearby, which first reduce the C–H bond strength and, secondly, provide favourable bonding situations for the resulting C–C fragments. The first function could be fulfilled by atoms in the flat surface also, as our calculations have shown.

Acknowledgements

We thank Prof. Dr. P. Ros, Dr. E.J. Baerends and Dr. J.G. Snijders for making available and for assistance in using the HFS–LCAO program.

Part of this work has been performed at the CECAM workshop "Models and Numerical Methods for the Study of the Structure of Surfaces and Adsorbates on Surfaces", held in Orsay in July and August 1977. One of us (P.G.) thanks Dr. C. Moser for his hospitality. We are also grateful to Dr. J.E. Demuth for stimulating discussions and for making available his results prior to publication.

The investigations were supported in part by the Netherlands Foundation for Chemical Research (SON) with financial aid from the Netherlands Organization for the Advancement of Pure Research (ZWO).

References

[1] L. Whalley, B.J. Davis and R.L. Moss, Trans. Faraday Soc. 67 (1971) 2445.
[2] M.K. Al-Noori and J.M. Saleh, J. Chem. Soc. Faraday I, 69 (1973) 2140.
[3] C.R. Brundle, Faraday Discussions 58 (1974) 138.
[4] J.E. Demuth and D.E. Eastman, Phys. Rev. Letters 32 (1974) 1123.
[5] J.E. Demuth, Surface Sci. 69 (1977) 365.
[6] J.E. Demuth, Phys. Rev. Letters 40 (1978) 409.
[7] J.E. Demuth, IBM J. Res. Develop. 22 (1978) 265.
[8] G. Casalone, M.G. Cattania, M. Simonetta and M. Tescari, Surface Sci. 62 (1977) 321.
[9] M.G. Cattania, M. Simonetta and M. Tescari, Surface Sci. 82 (1979) L615.
[10] J.C. Hemminger, E.L. Muetterties and G.A. Somorjai, J. Am. Chem. Soc. 101 (1979) 62.
[11] J.C. Bertolini, J. Massardier and G. Dalmai-Imelik, J. Chem. Soc. Faraday I 74 (1978) 1720.
[12] J.C. Bertolini and J. Rousseau, Surface Sci. 83 (1979) 531.
[13] J.E. Demuth and H. Ibach, Surface Sci. 78 (1978) L238.

[14] J.E. Demuth and H. Ibach, Surface Sci. 85 (1979) 365.
[15] S. Lehwald, W. Erley, H. Ibach and H. Wagner, Chem. Phys. Letters 62 (1979) 360.
[16] S. Lehwald and H. Ibach, Surface Sci. 89 (1979) 425.
[17] J.E. Demuth and D.E. Eastman, Phys. Rev. B13 (1976) 1523.
[18] J.E. Demuth, Surface Sci. 84 (1979) 315.
[19] T.H. Upton and W.A. Goddard III, J. Am. Chem. Soc. 100 (1978) 321.
[20] H. Itoh and A.B. Kunz, Chem. Phys. Letters 66 (1979) 531.
[21] A.B. Anderson, J. Chem. Phys. 65 (1976) 1729.
[22] A.B. Anderson, J. Am. Chem. Soc. 100 (1978) 1153.
[23] H. Kobayashi, H. Kato, K. Tarama and K. Fukui,J. Catalysis 49 (1977) 294.
[24] R.V. Kasowski, Surface Sci. 63 (1977) 370.
[25] W.C. Swope and H.F. Schaefer III, J. Am. Chem. Soc. 98 (1976) 7962.
[26] W.C. Swope and H.F. Schaefer III, Mol. Phys. 34 (1977) 1037.
[27] A.B. Anderson, J. Am. Chem. Soc. 99 (1977) 696.
[28] T.N. Rhodin, C.F. Brucker and A.B. Anderson, J. Phys. Chem. 82 (1978) 894.
[29] A. Gavezzotti and M. Simonetta, Chem. Phys. Letters 48 (1977) 434.
[30] R.C. Baetzold, Chem. Phys. 38 (1979) 313.
[31] E.J. Baerends, D.E. Ellis and P. Ros, Chem. Phys. 2 (1973) 41.
[32] E.J. Baerends and P. Ros, Chem. Phys. 2 (1973) 52.
[33] E.J. Baerends and P. Ros, Intern. J. Quantum Chem. S12 (1978) 169; and references therein.
[34] P. Geurts and A. van der Avoird, papers II, III and IV in this series, to be published.
[35] J.C. Slater, Quantum Theory of Molecules and Solids, Vol. 4 (McGraw-Hill, New York, 1974).
[36] J.G. Snijders and E.J. Baerends, Mol. Phys. 33 (1977) 1651.
[37] P.J.M. Geurts, J.W. Gosselink, A. van der Avoird, E.J. Baerends and J.G. Snijders, Chem. Phys. 46 (1980) 133.
[38] E. Clementi and C. Roetti, Atomic Data and Nuclear Data Tables, Vol. 14 (Academic Press, New York, 1974) p. 177.
[39] K.H. Johnson, Annu. Rev. Phys. Chem. 26 (1975) 39.
[40] R.S. Dickson and J.A. Ibers, J. Organomet. Chem. 36 (1972) 191.
[41] Y. Wang and P. Coppens, Inorg. Chem. 15 (1976) 1122.
[42] O.S. Mills and B.W. Shaw, J. Organomet. Chem. 11 (1968) 595.
[43] V.W. Day, S.S. Abdel-Meguid, S. Dabestani, M.G. Thomas, W.R. Pretzer and E.L. Muetterties, J. Am. Chem. Soc. 98 (1976) 8289.
[44] J.L. Davidson, M. Green, F.G.A. Stone and A.J. Welch, J. Am. Chem. Soc. 97 (1975) 7490.
[45] M.G. Thomas, E.L. Muetterties, R.O. Day and V.W. Day, J. Am. Chem. Soc. 98 (1976) 4645.
[46] R.S. Dickson, H.P. Kirsch and D.J. Lloyd, J. Organomet. Chem. 101 (1975) C48.
[47] L.F. Dahl and D.L. Smith, J. Am. Chem. Soc. 84 (1962) 2450.
[48] L.L. Kesmodel, P.C. Stair, R.C. Baetzold and G.A. Somorjai, Phys. Rev. Letters 36 (1976) 1316.
[49] L.L. Kesmodel, R.C. Baetzold and G.A. Somorjai, Surface Sci. 66 (1977) 299.
[50] H. Ibach and S. Lehwald, J. Vacuum Sci. Technol. 15 (1978) 407.
[51] T.E. Fischer and S.R. Kelemen, Surface Sci. 74 (1978) 47.
[52] R.C. Weast, Ed., Handbook of Chemistry and Physics, 55th ed. (CRC Press, Cleveland, 1974) pp. F-200–201.
[53] M.J.S. Dewar, Bull. Soc. Chim. Franc. 18 (1951) C79.
[54] J. Chatt and L.A. Duncanson, J. Chem. Soc. (1953) 2939.
[55] H.C. Allen, Jr. and E.K. Plyler, J. Am. Chem. Soc. 80 (1958) 2673.

[56] T. Ziegler and A. Rauk, Theoret. Chim. Acta 46 (1977) 1.
[57] E.J. Baerends and P. Ros, Mol. Phys. 30 (1975) 1735.
[58] R.S. Mulliken, J. Chem. Phys. 23 (1955) 1833.
[59] R.S. Mulliken, J. Chem. Phys. 23 (1955) 1841.
[60] D.W. Turner, C. Baker, A.D. Baker and C.R. Brundle, Molecular Photoelectron Spectroscopy (Wiley, London, 1970).
[61] T. Koopmans, Physica 1 (1934) 104.
[62] A. Rosén, E.J. Baerends and D.E. Ellis, Surface Sci. 82 (1979) 139.
[63] T.E. Fischer, S.R. Kelemen and H.P. Bonzel, Surface Sci. 64 (1977) 157.
[64] D. Dolphin and A. Wick, Tabulation of Infrared Spectral Data (Wiley, New York, 1977) p. 74.
[65] D.E. Ellis, E.J. Baerends, H. Adachi and F.W. Averill, Surface Sci. 64 (1977) 649.
[66] L. Pauling, The Nature of the Chemical Bond, 3rd ed. (Cornell University Press, Ithaca, NY, 1960) p. 260.
[67] J.E. Demuth, H. Ibach and S. Lehwald, Phys. Rev. Letters 40 (1978) 1044.